VECTOR MESON MASSES IN THE NUCLEAR MEDIUM

G.E. BROWN*

State University of New York at Stony-Brook, Department of Physics
Stony-Brook, NY 11794, USA

M. RHO

Service de Physique Théorique, CE de Saclay
F-91191 Gif-sur-Yvette Cedex, France

AND

MADELEINE SOYEUR

Laboratoire National Saturne, CE de Saclay
F-91191 Gif-sur-Yvette Cedex, France

(Received September 8, 1992)

Dedicated to Janusz Dąbrowski in honour of his 65th birthday

The decrease of vector meson masses with the pion decay constant for increasing baryon density, $m_V^*/m_V = f_\pi^*/f_\pi$, is related to scaling properties of the Skyrme Lagrnagian. Experimental data sensitive to vector meson properties in nuclei, such as K^+ scattering and (e,e',p) reactions, are shown to be compatible with the above relation.

PACS numbers: 21.65. +f, 11.40. Fy

1. Introduction

The idea that the vector meson masses ($m_V = m_\rho, m_\omega$) decrease in medium at about the same rate as the nucleon *effective* mass, *i.e.*,

$$\frac{m_V^*(\rho)}{m_V} \approx \frac{m_N^*(\rho)}{m_N}, \tag{1.1}$$

* Supported in part by the U.S. Department of Energy under Grant No DE-FG02-88 ER 4038.

has been suggested in a number of papers, the arguments being economically summarized in Ref. [1]. In this reference, Brown and Rho rewrote the Skyrme Lagrangian, which we here consider in the chiral limit (bare quark masses equal to zero),

$$\mathcal{L} = \frac{f_\pi^2}{4} \operatorname{Tr}\left(\partial_\mu U \partial^\mu U^+\right) + \frac{\varepsilon^2}{4} \operatorname{Tr}\left[U^+\partial_\mu U, U^+\partial_\nu U\right]^2 , \tag{1.2}$$

so that it was consistent with the scaling properties of the QCD action. Here f_π is the pion decay constant, U is the Sugawara variable,

$$U(x) = \exp\left(i\frac{\vec{\tau}\cdot\vec{\pi}}{f_\pi}\right) , \tag{1.3}$$

and we shall discuss ε^2 later. Following Campbell *et al.* [2], the correct scaling property in the first term was restored by multiplying f_π^2 by $(\chi/\chi_0)^2$, where χ is the glueball field, and χ_0 is its value at zero density. An additional term,

$$\delta\mathcal{L}_\chi = \tfrac{1}{2}\partial_\mu\chi\partial^\mu\chi + V(\chi) , \tag{1.4}$$

made the χ a dynamical field. The $V(\chi)$ can then be chosen to explicitly break scale invariance so as to mimic the way that quantum corrections break it in QCD. The χ field was then written as

$$\chi = \chi_* + \chi' , \tag{1.5}$$

where χ_* is the glueball mean field. Only χ_* was retained in the consideration of hadrons composed of the light up and down quarks. In this way, f_π^2 in Eq. (1.2) was replaced by

$$f_\pi^2 \to f_\pi^{*2} \equiv f_\pi^2\left(\frac{\chi_*}{\chi_0}\right)^2 . \tag{1.6}$$

The modified Skyrme Lagrangian then possesses only the scale f_π^*. Consequently, when the nucleon emerges as a soliton from this modified Lagrangian, its mass m_N^* scales as

$$\frac{m_N^*}{m_N} = \frac{f_\pi^*}{f_\pi} . \tag{1.7}$$

The m_N^* is to be identified as the *effective* mass of the nucleon; *i.e.*, the quasiparticle velocity for a nucleon of momentum p is

$$v_{QP} = \frac{p}{m_N^*} . \tag{1.8}$$

For simplicity, we do not introduce vector mean fields, which contribute to the nucleon energy; these would not change our argument.

If we work, as in Ref. [1], at the mean field level with axial vector coupling $g_A = 1$, the coefficient ε^2 of the Skyrme fourth order term is [3]

$$\varepsilon^2 = \frac{f_\pi^2}{4m_V^2} . \tag{1.9}$$

(Of course, loop corrections, which increase g_A, may modify our results.) Since the fourth order term involves four derivatives, it is already scale invariant, so ε^2 does not change with density. This implies that

$$\frac{f_\pi^*}{f_\pi} = \frac{m_V^*}{m_V} , \tag{1.10}$$

i.e., that the vector meson mass scales with f_π. Since f_π^* is the order parameter for the broken symmetry mode of chiral symmetry, this shows that m_V^* can equally well be used as order parameter. In fact, in justifying the procedure of [1] starting form the QCD sum rules, this proved to be convenient [4].

Whereas we believe the above considerations to establish that the vector meson mass m_V should decrease with density, it is of interest to consider what this scaling implies for experiments.

In a first application [5] to K^+ scattering by ^{12}C, it was found that the decreased $m_V^*(\rho)$ could explain the fact that the experimentally measured ratio of cross sections,

$$\frac{\sigma(K^+, {}^{12}C)}{\sigma(K^+, {}^{2}D)} \geq 6 , \tag{1.11}$$

was greater than given by the impulse approximation. This was because the vector meson propagators $(m_V^{*2}(\rho) + q^2)^{-1}$ were increased by the decreased mass. More importantly, the density dependence of $m_V^*(\rho)$ changed slightly that of the optical model potential, and allowed a reconciliation between the nucleon charge distributions used in K^+ and electron scattering from ^{12}C. In a similar vein, introduction of dropping masses was found to remove a long-standing nuclear radius discrepancy in the scattering of several hundred MeV protons by nuclei [6].

Although the drop in vector meson masses tends to increase the $(K^+, {}^{12}C)$ scattering cross section, it decreases the longitudinal response in (e,e'p) and (e,e') reactions [7]. The mechanism for this decrease can be understood by considering the vector dominance model, by which the virtual γ-ray from the electron scattering couples to the nucleon through the vector meson. The propagator for the latter is

$$D(V) = \frac{m_V^2}{m_V^2 + q^2} = \frac{1}{1 + q^2/m_V^2} , \tag{1.12}$$

with approximation to space-like momentum transfer q. The m_V^2 in the numerator, which technically can be considered to be a subtraction, is necessary to ensure that as $q^2 \to 0$, the correct electron charge e enters into reaction. In the case of finite density, $m_V \to m_V^*$ and

$$D(\omega) \to \frac{1}{1 + q^2/m_V^{*2}} . \tag{1.13}$$

Since $m_V^* < m_V$, this represents a *decrease* in $D(\omega)$ and a decrease in the longitudinal response. In the case of transverse response, an additional $(m_N^*)^{-1}$ enters in through the magnetic current coupling of the virtual γ-ray to nucleons [8], as we show later, largely cancelling this decrease.

The above somewhat schematic arguments indicate that scaling of vector meson masses affects the operators entering into electron scattering off nuclei in such a way to qualitatively explain discrepancies between experiment and theory. Since detailed and accurate data on separated longitudinal and transverse response exist for several nuclei with varying average densities, it is of interest to see to what extent theoretical models incorporating density dependent vector meson masses fit these data quantitatively. This was the object of the work of Ref. [9]. In this note we summarize the main points of this detailed work.

2. In-medium electromagnetic form factors in the two-phase model of the nucleon

In Ref. [9] the most complete model considered was the two-phase chiral model; *i.e.*, a quark core surrounded by a nonperturbative meson cloud (soliton cloud). In many calculations, this model has been employed with a fixed radius of $R \lesssim 0.5$ fm, separating quarks and meson cloud. It is more usual in QCD to change from nonperturbative to perturbative descriptions in, *e.g.*, calculation of loop corrections, in momentum space, at a momentum

$$\Lambda_{\chi^{SB}} \simeq 1 \text{ GeV} , \tag{2.1}$$

(where the notation χ^{SB} stand for "chiral symmetry breaking") rather than in coordinate space. Since a wide range of momenta were considered in Ref. [9], it was necessary to implement the change, and this was done by introducing bag radii R which increased with increasing momenta. The coupling of photons to nucleons in the two phase picture results from two mechanisms, a direct coupling to the charge of quarks in the quark core and a coupling through vector mesons to the (soliton) meson cloud. At momenta somewhat higher them $\Lambda_{\chi^{SB}}$ the effects from the meson cloud, which are

important for us here, should go away and the picture should go over to one of scattering by the (perturbative) quark structure of the nucleon. Thus, our model should be restricted to momenta $q < \Lambda_{\chi \mathrm{SB}}$.

Within this domain of momenta $|q| < \Lambda_{\chi \mathrm{SB}}$, a schematic model illustrates simply the main results of our two-phase model. In this model, isoscalar operators couple equally to quark and meson sectors, whereas isovector operators couple only to the meson cloud. This approximation is justified in Ref. [9] and approximately follows the way in which isoscalar and isovector charges fraction in the chiral hyperbag model [10]. Our schematic model is similar to that used in Refs [7] and [8]. For completeness, a purely solitonic model with $R = 0$ is also used. The difference in predictions between these models may give some idea of the model dependence of our results.

We employ the expressions introduced in [7] for the bag and meson form factors $F_{\mathrm{B}}(q^2)$ and $F_{\mathrm{M}}(q^2)$. The bag form factor is given by

$$F_{\mathrm{B}}(q^2) = \frac{1}{1 - q^2/\lambda^2}\,, \tag{2.2}$$

in which λ^2 is related to the bag radius by [10]

$$\frac{6}{\lambda^2} = \frac{3}{5}R^2\,. \tag{2.3}$$

That part of the coupling of the γ-ray to the nucleon through the vector meson involves the product of a hadronic form factor with the vector meson propagator,

$$F_{\mathrm{M}}(q^2) = \frac{\Lambda^2 - m_V^2}{\Lambda^2 - q^2}\frac{m_V^2}{m_V^2 - q^2}\,, \tag{2.4}$$

the propagator having been discussed earlier, Eq. (1.12). Here Λ^2 is a cutoff for which we assume the value $\Lambda^2 = 2m_V^2$ [7]. The $F_{\mathrm{M}}(q^2)$ is then multiplied by the fraction of the charge in the meson cloud. As noted earlier and as shown in [9, 10], the fractionation is such that substantially more of the isovector charge is in meson cloud. This is the basis of our schematic model.

The longitudinal response measures the charge density and, therefore, the operator is

$$O^{\mathrm{L}} = \tfrac{1}{2} + \tfrac{1}{2}\tau_3\,. \tag{2.5}$$

The transverse response measures the current density and the corresponding operator is of the form

$$O^{\mathrm{T}} = \mu_V \frac{\varepsilon[\boldsymbol{\sigma} \times \boldsymbol{q}]}{2m_N}\tau_3\,, \tag{2.6}$$

where ε is the polarization vector of the virtual γ-ray and μ_V is the isovector moment

$$\mu_V = \tfrac{1}{2}(\mu_p - \mu_n) = 2.353\,. \tag{2.7}$$

We neglect the much smaller isoscalar component of the current. We believe our nonrelativistic expressions for charge and current density to be adequate for the momentum range of $q \lesssim 500 - 600$ MeV/e in which comparison of our theoretical estimates with data is most significant.

At nuclear matter density we take

$$\frac{m_N^*(\rho_0)}{m_N} = 0.8 \tag{2.8}$$

and extrapolate linearly from ρ_0 to zero by

$$\frac{m^*(\rho)}{m} = 1 - 1.176\rho(\mathrm{fm}^{-3}) \tag{2.9}$$

for all masses ($m = m_N, m_\omega, m_\rho$).

From the operators (2.5) and (2.6), we can easily see why the longitudinal response is, compared with shell model value, smaller than the transverse one. The O^{T} has an m_N in the denominator, which is not present in O^{L}. This m_N goes to $m_N^* < m_N$ *in medium* and this increases the transverse response relative to longitudinal. Thus, the relative increase in transverse response stems from a particularly simple effect.

3. Longitudinal and transverse response functions measured in (e,e') and in (e,e' p) reactions

The separation of the electron scattering into longitudinal and transverse components is discussed in Ref. [9] and in many other places, so we shall simply show separated data and compare them with our theoretical models.

In Fig. 1 we show the transverse and longitudinal response functions for the (e,e') reaction on ^{40}Ca from [11], compared with an independent particle calculation. Whereas $\sim 30\%$ of the longitudinal strength from this calculation appears to be missing, the calculation does well for the transverse response. In our model, the decrease in meson propagators is exactly compensated for at this moment transfer by the enhancement in the operator O^{T}, Eq. (2.6), due to decreased m_N^*.

In Fig. 2 we show the q-dependence of the transverse and longitudinal cross sections for the (e,e',p) reaction on a bound proton in ^{40}Ca. The curves are divided by the independent particle expectations, as calculated in [12]. The theoretical curves here, and in the following figures are obtained:

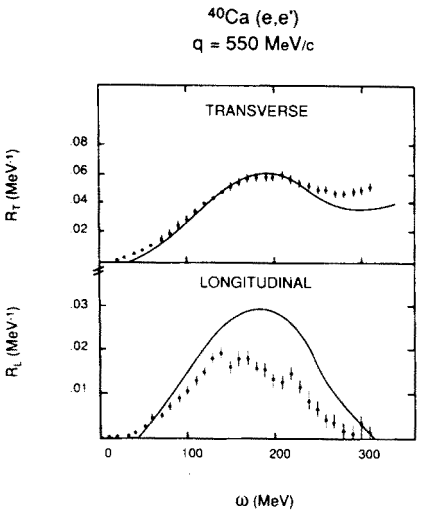

Fig. 1. Transverse and longitudinal response functions for the (e,e′) reaction on ^{40}Ca (from Ref. [11]). The solid line is an independent particle calculation.

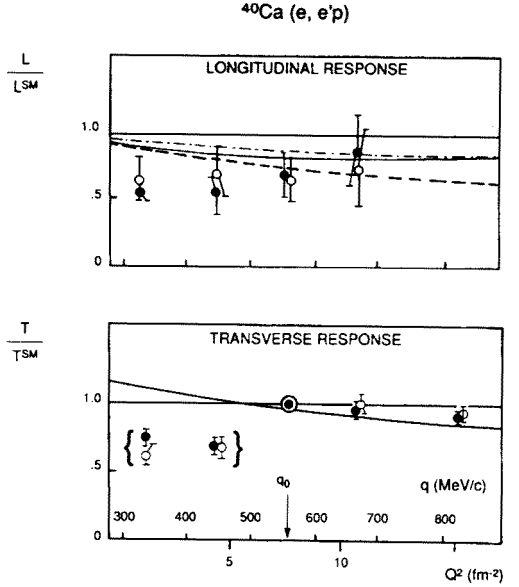

Fig. 2. q-dependence of the transverse and longitudinal cross sections for a bound proton in ^{40}Ca divided by independent particle expectations (from Ref. [12]). The bracketed points are taken in kinematic conditions corresponding to the dip region and therefore excluded from the one-body analysis. The theoretical curves are obtained with density dependent vector meson masses using the prescription for the q-dependence of the nucleon structure described in Ref. [9] (solid line), a soliton without quark core (dashed line) and a model where the isoscalar photon coupling is 50% to the quarks and 50% to the soliton cloud (dot-dashed line).

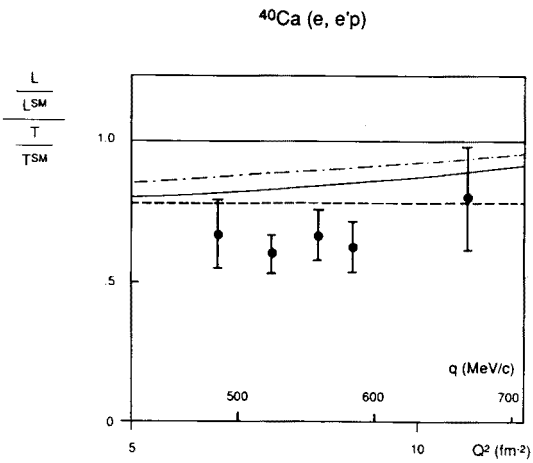

Fig. 3. q-dependence of the ratio of the longitudinal to transverse responses for a bound proton in ^{40}Ca normalized by independent particle predictions (from Ref. [12]). The meaning of the theoretical curves is the same as in Fig. 2

(i) Solid line: with density dependent meson and nucleon effective masses and the q-dependence of the nucleon structure described in Ref. [9].

(ii) Dot-dashed line: with density dependent masses and schematic isoscalar photon coupling of 50% to the quarks, 50% to the meson cloud, isovector coupling 100% to the cloud.

(iii) Dashed line: density dependent masses and soliton without quark core.

Although the inclusion of density dependent masses removes much of the discrepancy between theory and experiment in the case of the longitudinal response, the latter seems to be systematically below our theory. Indeed, the problem of missing longitudinal strength is a well known one, and a substantial part of it can be explained in terms of standard many-body correlations in nuclei [13]. These cannot explain all of the missing strength, and the conclusion of Alberico *et al.* [13] is "However, in order to attain the right magnitude we had to introduce a *modified* proton form factor corresponding to an electromagnetic radius larger by about 20% (in ^{40}Ca and ^{56}Fe) with respect to the free case." Of course our decrease in effective mass to $m_N^* = 0.8 m_N$ increases the scale of the meson sector, which is chiefly responsible for the low-energy longitudinal electron scattering, so our conclusions are consistent with the results of [13].

It is constructive in Fig. 3 to plot the q-dependence of the ratio of longitudinal to transverse responses for a bound proton in ^{40}Ca, normalized by independent particle predictions from Ref. [11]. The meaning of the theoretical curves is the same as in Fig. 2.

We next consider ^{4}He and ^{3}He, in which two-particle, two-hole correc-

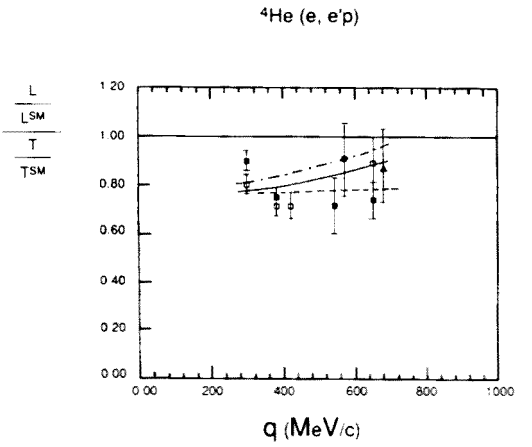

Fig. 4. Same as Fig. 3 for ^{4}He. The different symbols correspond to different missing momenta p_m (p_m is the momentum of the undetected system). The open squares, the closed squares and the closed triangle correspond to p_m = 30 MeV/c, 90 MeV/c and 190 MeV/c respectively (from Ref. [14]).

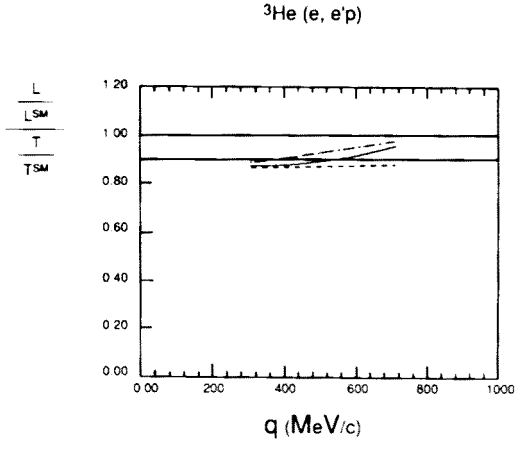

Fig. 5. Ratio of the longitudinal to transverse responses for a bound proton in ^{3}He normalized by independent particle predictions. The average experimental effect of a 10% reduction is indicated by a full horizontal line at $(L/L^{SM})/(T/T^{SM}) = 0.9$ (from Ref. [15]). The meaning of the theoretical curves is the same as in Fig. 3.

tions, *etc.*, should be relatively unimportant. In Figs 4 and 5 we show ratios of longitudinal and transverse responses [14, 15], compared with theoretical models. In Fig. 5 the average experimental effect of a 10% reduction is indicated by a full horizontal line at $(L/L^{SM})/(T/T^{SM}) = 0.9$ [15].

According to our scaling of masses (2.9), the ratio $(L/L^{SM})/(T/T^{SM})$ should go roughly linearly with density. In Fig. 6 we show the density

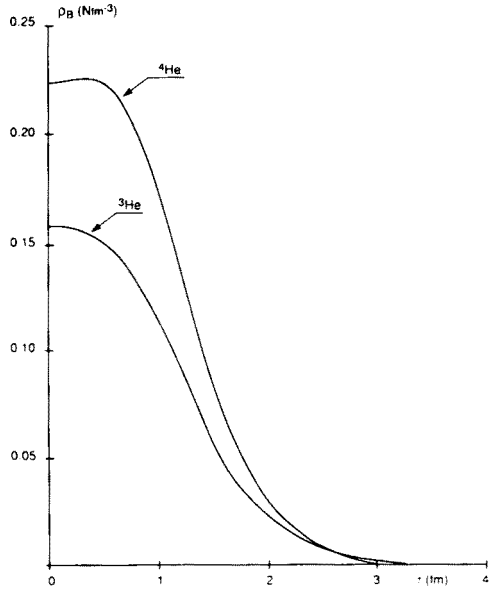

Fig. 6. Matter densities of ^{3}He and ^{4}He (from Ref. [16]).

distributions in ^{4}He and ^{3}He [16]. We note that the 1.5 to 2 times larger experimental difference of the above ratio from unity in ^{4}He, as compared with ^{3}He, is compatible with the ratio of densities.

4. Conclusions

Our chief conclusion is that the scaling law

$$\frac{m_N^*(\rho)}{m_N} = \frac{m_V^*(\rho)}{m_V}, \tag{4.1}$$

is compatible with the Saclay (e,e'p) data. Indeed, introduction of this scaling improves the agreement between theory and data, although additional correction for multiparticle correlations appears to be needed in the ^{40}Ca longitudinal response.

The reduction in the longitudinal response seems to generally follow the linear density dependence implied by (4.1). However, error bars in the data and uncertainties in their interpretation do not allow definite and quantitative conclusions. None the less, we find it encouraging that the introduction of scaling meson masses for which there is by now the rather compelling theoretical motivation outlined in Section 1, induces changes in such a way as to improve agreement between theory and experiment.

Our treatment of the vector mesons has been somewhat schematic. In particular, we treated the ρ-meson in zero-width approximation, whereas it is known to have a rather rich structure in spectral composition, including a substantial two-pion continuum. The distribution in spectral strength will change *in medium.* A recent calculation [17] shows that a new structure corresponding to the decay of the ρ-meson into a pion-like and a ΔN^{-1}-like mode, arises around $M = 3m_\pi$. In this calculation the ρ-mass is included in a term

$$\delta\mathcal{L} = \tfrac{1}{2}(m_\rho^o)^2 \rho_\mu \rho^\mu , \tag{4.2}$$

in the Lagrangian, where m_ρ^o is treated as a constant, independent of density. The effect we discuss in this note amounts to replacing m_ρ^o by $m_\rho^{*o}(\rho)$; *i.e.*, making the bare ρ-meson mass a function of density. Our effect could easily be incorporated in the calculations. Basically, it arises from the change in vacuum condensate with density. This change is not included in the calculations of [17], which deal with standard many body effects concerned with coupling of pions to nucleons, *etc.* Thus, there is no double counting combining the two effects.

One of us (G.E.B.) would like to thank Magda Ericson for helpful discussions of the matters in this paper. He would also like to recall a friendship with Janusz Dąbrowski that began three and a half decades ago.

REFERENCES

[1] G.E. Brown, M. Rho, *Phys. Rev. Lett.* **66**, 2720 (1991).
[2] B.A. Campbell, J. Ellis, K.A. Olive, *Nucl. Phys.* **B345**, 325 (1990).
[3] I. Zahed, G.E. Brown, *Phys. Rep.* **142**, 1 (1986).
[4] C. Amadi, G.E. Brown, *Phys. Rev.* **D46**, 478 (1992).
[5] G.E. Brown, C.B. Dover, P.B. Siegel, W. Weise, *Phys. Rev. Lett.* **60**, 2723 (1988).
[6] G.E. Brown, A. Sethi, N. Hintz, *Phys. Rev.* **C44**, 2653 (1991).
[7] G.E. Brown, M. Rho, *Phys. Lett.* **B222**, 324 (1989).
[8] G.E. Brown, M. Rho, *Phys. Lett.* **B237**, 3 (1990).
[9] M. Soyeur, G.E. Brown, M. Rho, *Nucl. Phys.* **A**, to be published.
[10] B.-Y. Park, M. Rho, *Z. Phys.* **A331**, 151 (1988).
[11] Z.E. Meziani *et al.*, *Phys. Rev. Lett.* **52**, 2130 (1984); D. Reffay-Pikeroen, Thesis, Orsay, July 1987.
[12] D. Reffay-Pikeroen *et al.*, *Phys. Rev. Lett.* **60**, 776 (1988).
[13] W.M. Alberico, P. Czerski, M. Ericson, A. Molinari, *Nucl. Phys.* **A462**, 269 (1987); V.R. Pndharipande, *Proc. of Dronten Summer School*, ed. P.K.A. de Witt-Huberts, 1990.

[14] A. Magnon *et al.*, *Phys. Lett.* **B222**, 352 (1989); J.-E. Ducret *et al.*, to be published.
[15] L. Lakehal-Ayat *et al.*, to be published; Also *Contribution to the 5th Workshop on Perspectives in NUclear Physics at Intermediate Energy*, Triest, May 1991.
[16] H. Phan Xuan, private communication.
[17] M. Herrmann, B.L. Friman, W. Nörenberg, Preprint GSI-92-15.